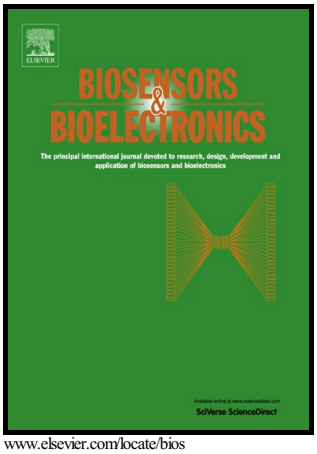

www.elsevier.com/locate/bios

Photoelectrochemical biosensor constructed using TiO_2 mesocrystals based multipurpose matrix for trypsin detection

Hong Dai, Yilin Li, Sihong Chen, Baoshan Zeng, Shupei Zhang, Zhengsheng Hong, Yanyu Lin

PII: S0956-5663(16)31035-1
DOI: http://dx.doi.org/10.1016/j.bios.2016.10.028
Reference: BIOS9250

To appear in: *Biosensors and Bioelectronic*

Received date: 29 May 2016
Revised date: 11 October 2016
Accepted date: 14 October 2016

Cite this article as: Hong Dai, Yilin Li, Sihong Chen, Baoshan Zeng, Shupe Zhang, Zhengsheng Hong and Yanyu Lin, Photoelectrochemical biosenso constructed using TiO_2 mesocrystals based multipurpose matrix for trypsi detection, *Biosensors and Bioelectronic* http://dx.doi.org/10.1016/j.bios.2016.10.028

Photoelectrochemical biosensor constructed using TiO_2 mesocrystals based multipurpose matrix for trypsin detection

Hong Dai,[a*] Yilin Li,[a] Sihong Chen,[a] Baoshan Zeng,[a] Shupei Zhang,[a] Zhengsheng Hong,[b**] Yanyu Lin[c]

a College of Chemistry and Chemical Engineering, Fujian Normal University, Fuzhou 350108, P. R. China

b Fujian Provincial Key Laboratory of Quantum Manipulation and New Energy Materials, College of Physics and Energy, Fujian Normal University, Fuzhou 350108, P. R. China

c Ministry of Education Key Laboratory of Analysis and Detection for Food Safety, and Department of Chemistry, Fuzhou University, Fuzhou 350002, P. R. China

Corresponding author

Fax: (+86)-591-22866135;

E-mail: dhong@fjnu.edu.cn (H. Dai);

winter0514@163.com (Z. Hong)

Abstract

Herein, a delicate photoelectrochemical biosensor for quantitative detection of trypsin was successfully established by virtue of polyethylenimine-sensitized TiO_2 mesocrystal as the photoactive matrix integrated with Boron-doped carbon quantum dots labeled peptide as the signal amplification tags. Specifically, polyethylenimine with fine photo-stability was introduced here as the electron transporting layer to reduce the energy barrier of TiO_2 mesocrystal, thereby facilitating the carriers transfer and improving the photocurrent response. Moreover, the Boron-doped carbon dots-peptide bioconjugates could noticeably decrease the photocurrent due to the competitively light harvesting by Boron-doped carbon dots and the steric hindrance of peptide chains, leading to less light energy arriving at the TiO_2 mesocrystal and hindering the electrons transfer between the electrolyte and electrode. The anchored conjugates synergistically promoted the decline of photocurrent signal, evidently enhancing the sensitivity of this detection protocol. When trypsin was incubated, the photoelectric signal was obviously re-promoting because arginine-containing peptide chains could be specifically cleaved by trypsin and the Boron-doped carbon quantum dots was affranchised from the electrode, making the most of the previous suppression effects released. Therefore, the intensity of photocurrent signal was proportional to the trypsin concentration in a wide linger range from 1×10^{-7} mg/mL to 1.0 mg/mL. This practical and elegant "on-off-on" biosensor with high sensitivity offered a promising scheme to monitor various proteases and the inhibitors screening for early diagnoses of different diseases.

Keywords: Photoelectrochemical biosensor, TiO_2 mesocrystals, Boron-doped carbon quantum dots, Trypsin

1. Introduction

Photoelectrochemical (PEC) sensing, a new-type and promising analytical tool based on the exquisitely constructed photo-electrodes that convert photo-irradiation to electrical signal, offers a powerful way in the fields of clinical diagnostics, environmental monitoring, and food safety (Yan et al. 2015; Zhao et al. 2014). Benefiting from the entire separation of detection signal and excitation source, its sensitivity is higher than the electrochemical methods owing to the greatly reduced background signal (Ge et al. 2013). Prevalently, considerable attention has been drawn to the construction of efficient biosensor with simplicity for protein detection in medical diagnostics and pathogen recognition for early intervention and better management of ailments. Trypsin is one of the necessary digestive enzymes produced by pancrea, controlling the pancreatic exocrine function. Moreover, massive diseases are correlated to the change of trypsin levels, for instance, cystic fibrosis, pancreatitis, necrosis, and meconium ileus (Zhang et al. 2014). Therefore, fabricating a delicate bioassay for trypsin and its inhibitor monitoring is beneficial for therapeutic implications. Hitherto, a host of techniques containing enzyme-linked immunosorbent assays (Rhodes et al. 1957), electrochemistry (EC) (Chen et al. 2012) and fluorescence (FL) spectroscopy (Hong et al. 2014; Zheng et al. 2012) were fabricated for trypsin test. However, the sensitivity of these methods was supposed to be further enhanced, and exploring a well-defined sensing platform with low background signal, well reproducibility, and wide response range was still an urgent requirement for trypsin determination. Up to present, the PEC assay designed for trypsin activity evaluation was reported rarely, and this technique avoided the expensive optical equipment and high potential in EC measurements.

In the PEC sensing system, selecting proper photoactive materials with

high-performance is a basic requirement, which provides a substantial momentum in enhancing photoelectrical response that sensitively reflecting the concentration of the target. Nowadays, TiO_2-based nanostructures have ignited massive research interests for a diverse range of applications due to its unique photoactivity, nontoxicity, and superior chemical and physical stability, thus making them prime candidates for photocatalytic and PEC scopes (Chen et al. 2014). TiO_2 mesocrystals, a newly typical class of superstructure material, composed of aligned nanoparticles with subunit alignment, periodically hierarchical structure, and high porosity, which notably enhanced the PEC performance (Zhou et al. 2007). Herein, the octahedral anatase mesocrystal (OAM) was synthetized through a facile and additive-free method under solvothermal conditions. However, the poor visible light absorption and fast charge carriers recombination impede the potential applications of TiO_2 mesocrystal (Li et al. 2013). To further improve the photo-response of OAM, the conjugated polyelectrolyte (CP) was introduced here to elevate the PEC performance. CP has been extensively applied for chemical and biological detections due to the large absorption cross sections and good photo-stability (Wang et al. 2015). Herein, the obtained OAM substrate with high porosity was covered with interlayer film of polyethylenimine (PEI) to achieve high efficiency of optical-to-electrical power conversion. The OAM was integrated with PEI through the mesoporosity absorption of OAM as well as the chelate effect that nitrogen atoms in PEI could combine with Ti (IV) surface site of OAM. Experimental outcomes have demonstrated that the OAM/PEI complexes owned significant merits, such as the enhanced electron mobility (Yang et al. 2014), reduced series resistance and improved charge separation, which obviously promoted the photocurrent intensity and stability. Additionally, PEI with amine group could be served as host matrix for following anchoring reaction. Representatively, the specific

recognition elements mainly include antibody, aptamer and peptide. In this work, synthetic peptides with various sequence motifs were used as trypsin substrates, which were important tools in various areas of biomedical research, diagnostics and pharmaceuticals development. So far, various chemical sensors have been prepared using proteases for cleaving peptide chains followed by appropriate signal transductions (Liu et al. 2014). Thus, a powerful PEC approach for sensitive bioassay was achieved here by utilizing the ‘‘on-off-on’’ strategy for trypsin detection. In addition to the initial amplified PEC signal based on OAM/PEI complexes, exploring an impactful quencher to assist the peptide chains and then synergistically depress the photocurrent response also held a vital position in this ‘‘on-off-on’’ PEC assay. Therefore, to further improve the sensitivity, an intriguing enzyme-free signal amplification tag was employed to label the peptide for indicating the signal change. Boron (B)-doped carbon quantum dots (B-CQDs) with good biocompatibility was a scalable carbon material that incorporated B atoms into carbon dots so as to change the electronic and chemical properties, with possible application in the field of biosensors. When B-CQDs were labeled on the arginine-containing peptide to form the Peptide@B-CQDs conjugates, the photocatalytic property of B-CQDs would competitively absorb the irradiating light and retard the carriers transfer between OAM/PEI system and the electrolyte, resulting in apparently weakened photocurrent intensity. Meanwhile, the steric hindrance of the bioconjugates also led to reduced photoresponse of this biosensing plateau. As B-CQDs and peptide synergistically promoted the decrease of photocurrent response, excellent analytical performance of the PEC bioassay could be accomplished. After incubated with active trypsin, partial peptide chains were cleaved and B-CQDs dropped from the electrode, causing an increased photocurrent signal. With the increment of trypsin amount, the detectable

signal improved.

Given the aforementioned conditions, a new-type “on-off-on” PEC biosensor was designed based on OAM/PEI complexes as PEC matrix coupled with Peptide@B-CQDs composition as efficient signal quencher for trypsin detection (Scheme 1). Initially, the bare glass carbon electrodes (GCE) were fabricated by stepwise modification of OAM and PEI. The formed OAM/PEI complexes provided significant advantages for improving light absorption and charge carries separation, which enhanced the photocurrent intensity and stability. Subsequently, the Peptide@B-CQDs conjugates were anchored through classic glutaraldehyde (GLD) cross linking reaction. This process seriously restrained the photocurrent response owing to the B-CQDs with high light absorption capability could competitively harvest the exciting light as well as the steric hindrance caused by bioconjugates inhibited the electrons migration between electrolyte and OAM/PEI complexes. Afterward, a short peptide fragment containing the B-CQDs was released away when trypsin was incubated on the electrode, leading to noticeably re-promoting photocurrent intensity. The photocurrent intensity was proportional to the amount of trypsin, and simultaneously the trypsin inhibitor efficacy could also be evaluated through this sensing system. This ‘‘on-off-on’’ strategy could overcome some drawbacks, such as the unneglected background response and the false positive PEC signal. The developed sensing platform provided a high sensitivity and a wide optional range for trypsin detection, which possessed enormous potential in high-throughput protease profiling applications.

Scheme 1

2. Experimental Section

2.1. Materials and reagents

Trypsin was obtained from the Ekear Biotechnology Co., Ltd. (Shanghai, China). Arginine-containing peptide (CAGRADADAD), Cys-Ala-Gly-Arg-Ala-Asp-Ala-Asp -Ala-Asp, was chosen as the model peptide that was purchased from the Karelay Biochem, Inc (China). Trypsin inhibitor, 1-ethyl-3-(3-(dimethylamino)propyl) carbodiimide (EDC), N-hydroxysuccinimide (NHS), PEI (99%, 10000), (3-Aminopropyl)triethoxysilane (APTEs) (98% purity), hydroquinone, and BBr_3 were obtained from Aladdin Chemistry Co., Ltd. (China). N, N-dimethylformamide (DMF) and GLD were attained from Sinopham Chemical Reagent Co., Ltd. (Shanghai, China). Other reagents were of analytical grade and all aqueous solutions were prepared using ultrapure water. Phosphate buffer solution (PBS) was acquired by mixing stock solution of 0.1 M Na_2HPO_4 and 0.1 M NaH_2PO_4 to adjust pH value. The OAM was synthetized according to the previous report (Dai et al. 2015), and the obtained production was dispersed in ultrapure water to prepare 10 mg/mL OAM suspension for future use.

2.2. Synthesis of B-CQDs and the preparation of Peptide@B-CQDs bioconjugates

B-CQDs were synthesized according to the previously published literature (Shan et al. 2014). Shorty, 2.1 g of hydroquinone, 10 mL of acetone and 5.16 mL of BBr_3 were laid into a 25 mL Teflon equipped with stainless steel autoclave, followed by heating solvothermally at 200 °C for 2 h in a blast oven. After the reaction finished, the autoclave was cooled to room temperature, and the solution was condensed through rotary evaporation. Finally, the achieved product was B-CQDs.

The Peptide@B-CQDs bioconjugates were prepared as follows. Firstly, 10 μL of B-CQDs (10 mg/mL) were dispersed in 50 μL of APTEs (wt. 1.0%) solution, stirred for 20 min and sonicated for 2 h. After that, the mixture was centrifuged for 15 min

with speed of 8000 rpm, and the sedimentation was re-dispersed in DMF to acquire the APTEs-functionalized B-CQDs for subsequent use. Meanwhile, 10 μL of aqueous solution containing 20 mg/mL of EDC and 10 mg/mL of NHS were added into 30 μL of peptide solution (10 mg/mL) for 4 h at 4 °C to active the carboxyl (-COOH) group of peptide. Subsequently, this mixed solution (40 μL) was placed into the as-prepared APTEs-functionalized B-CQDs solution (60 μL) and was gently shaken for 10 h at 4 °C. During this process, conjugation of Peptide@B-CQDs was acquired through the classic EDC/NHS coupling reaction between amine (-NH2) groups on the surface of B-CQDs and -COOH group of peptide. The unconjugated biomolecules of peptide were removed by centrifugation and washed with pH 7.4 PBS. Finally, the as-prepared Peptide@B-CQDs was re-dispersed into the PBS (100 μL).

2.3. Construction of the "on-off-on" PEC biosensor for trypsin detection

The steps for fabricating the biosensor were outlined in Scheme 1A. First, the suspension of OAM (4 μL, 1mg/mL) was dropped onto the freshly prepared GCE surface, dried at infrared lamp, and cooled to room temperature. Then the electrode was immersed into 0.5 mg/mL of PEI aqueous solution for 40 min to allow the sufficient absorption of PEI in the mesoporous OAM. After being dried at room temperature, 5 μL of GLD solution (5.0 wt.%) was thrown on the OAM/PEI modified electrode for 1 h at 4 °C, followed by a thorough rinsing with PBS (pH 7.4) to remove excess GLD. Then, the Peptide@B-CQDs was immobilized on the resulting electrode through the classical GLD cross linking reaction between the existing amine groups of PEI and peptide. After incubated for 1 h at 4 °C in 100% humidity, the electrodes were immersed into 20 μL of BSA (1.0 wt.%) for 1 h to prevent the nonspecific adsorption of peptide. After being washed with PBS (pH 7.4), the electrodes were employed as a PEC biosensor and incubated with 5 μL of activated trypsin standard

with different concentrations for 1 h at 37.5 °C. Following that, the modified electrode was washed with PBS (pH 7.4) and dried before measuring. The photocurrent was measured at the room temperature of 25 °C in pH 7.4 PBS with switchable light excitation at the applied potential of 0 V.

3. Results and Discussion

3.1. Morphology and composition characterization

Herein, a simple and additive-free strategy under solvothermal (acetic acid) conditions was provided to synthetize OAM. A series of characterizations were performed to explore the mesoporous TiO_2 structure. As shown in Fig. 1A, the scanning electron microscopy (SEM) image exhibited symmetrical and octahedral particles with the size of 40-100 nm in length, which formed mesoporous structures, making it selectively incorporate with the filling guest material inside host pore walls due to the enlarged contact area (Liu et al. 2010; Pan and Lee 2006). The Nitrogen adsorption-desorption was used to further verify the mesoporosity structure (manifested in inset of Fig. 1A). The sample displayed the isotherm of IV type with an apparent hysteresis loop, which was the representative of mesoporous structure. This outcome implied that the OAM structure was beneficial for the collection of photo-induced electrons and offered more reactive sites for intensive photocatalytic reaction and light harvest, resulting in an eminent PEC performance. Moreover, the microstructure of OAM was studied by high-resolution transmission electron microscopy (HRTEM) (presented in Fig. 1B). The clear lattice fringes with a spacing of 3.4 Å was submitted, well inosculating to the (101) planes in anatase structure. Following that, the X-ray diffraction (XRD) was performed to further certify the OAM phase structures (inset of Fig. 1B). The narrow sharp diffraction peaks at 2θ =25.3°, 37.8°, and 48.1° would be assigned to the (101), (004), and (200) planes of

anatase TiO_2, respectively, suggesting that the pure anatase TiO_2 with high crystalline was formed.

A facile, one-pot solvothemal route was performed to synthesize B-CQDs by utilizing boron tribromide (BBr_3) as the boron source and hydroquinone as the precursor (Shan et al. 2014). As presented in Fig. 1C, the HRTEM image indicated that B-CQDs also possessed crystalline lattice structures. Clear adjacent lattice plane of 2.1 Å was observed, demonstrating the graphene-like crystalline structure of B-CQDs, which was in agreement with the previous report (Shan et al. 2014). Additionally, the optical properties of B-CQDs were measured (submitted in Fig. 1D). The UV-vis spectra of the B-CQDs aqueous solution exhibited a broad and strong absorption from 300 to 500 nm, which indicated that the B-CQDs with high light absorbance was not favorable for OAM/PEI complex to harvest the light energy, thus weakening the photocurrent response of the OAM/PEI matrix. Besides, the FL spectra exhibited highly strong emission at ~598 nm when excited at 368 nm, implying that the photo-generated electrons and holes were extremely easy to recombine. The aforementioned phenomena revealed that B-CQDs were an efficient probe in enhancing the sensitivity of this PEC biosensor.

Fig. 1

3.2. Excellent PEC performance of OAM/PEI complexes

In this work, OAM with fine photocurrent response was used as the signal matrix, however, searching a flexible and cost-efficient sensitizer to improve the photoelectric performance of OAM was still a great challenge. Recently, amine-rich PEI has been applied in polymer solar cells (Kang et al. 2012) to promote the electrons transfer. During the formation of OAM/PEI layer, the spontaneous orientation of the ethylamine group in PEI caused the formation of permanent dipoles

(μ) at the OAM interface, which could reduce the work function of OAM by a downward vacuum level shift (Choi et al. 2011). Thus, the energy barrier for electron transport decreased with decreasing work function of OAM after depositing the PEI (Yang et al. 2014), thereby achieving an eminent photoelectric conversion efficiency. Several experiments were carried out here to certify this viewpoint. In Fig. 2A, the photocurrent densities of OAM (curve a) and OAM/PEI (curve b) were compared under chopped illumination. Notably, the curve b submitted a larger photocurrent density under the applied potentials from 0.1 V to 0.4 V, indicating that OAM/PEI owned a better PEC performance. Consistently, as shown in Fig. 2B, the incident photon-to-current conversion efficiency (IPCE) measurements were performed to elucidate the sensitizing effect of PEI at different wavelengths. The IPCE values obtained with no bias voltage was according to Eq. (1) (Kongkanand et al. 2008).

$$IPCE\% = (1240 \times j \times 100) / (\lambda \times P) \quad (1)$$

Where j, λ, and P were the photocurrent density in A cm^{-2}, wavelength of incident light in nm, and incident light power intensity in W cm^{-2}. Expectedly, the OAM/PEI complex presented an elevated photoresponse and IPCE value not only in the UV but also in the visible light region in comparison with pristine OAM, which derived from the work function decrement induced energy barrier decreasing in this complex.

Furthermore, the open-circuit photovoltage (Voc) response was performed to verify the prominent character of OAM/PEI complex, as shown in Fig. 2C. Under the light illumination, most of the photo-ignited electrons were accumulated in the OAM (curve a) or OAM/PEI (curve b) films, resulting in a shift of the Fermi level to a more negative voltage as well as the enhancement of the Voc (Chen et al. 2013). Subsequently, the Voc arrived at a stable status (maximum value) with the increase of

photo-generated electrons in these thin films. Once the irradiation was stopped, the Voc started to decline owing to the collected photoelectrons was recombined with photo-induced holes and scavenged by electron acceptor substances in solution (Song et al. 2008). The higher descend of Voc under light illumination and the tedious decay in dark jointly suggested the more effective charge separation and less recombination for OAM/PEI complex.

Lifetime of accumulated photoelectrons was estimated by monitoring the subsequent decay of photovoltage with time through the Eq. 2 (Bisquert et al. 2004).

$$\tau = \frac{k_B T}{e}\left(\frac{dV_{OC}}{dt}\right)^{-1} \quad (2)$$

Where τ was the potential dependent lifetime and the dV_{oc}/dt was the derivative of open-circuit voltage transient. The k_BT was the thermal energy in which T (K) was temperature and k_B was Boltzmann constant. The "e" in this formula was the charge of a single electron. As shown in Fig. 2D, the OAM/PEI complex exhibited prolonged decay lifetime of the photo-induced electrons. Through the above experiments, the comparison outcomes abundantly proved that the OAM/PEI (curve b) possessed remarkably increased photocurrent response compared to the pristine OAM.

Fig. 2

3.3. EIS and PEC characterization of the biosensor

Electrochemical impedance spectroscopy (EIS) was applied to evaluate the interface properties of the electrode (displayed in Fig. 3A). Each impedance spectrum composed a semicircle and a linear part that reflected the electron-transfer and the diffusion limited process, respectively. EIS Nyquist plots of GCE/OAM (curve b) presented a relatively larger electron-transfer resistance (Ret) compared with the bare GCE (curve a) as a result of weak conductivity of the OAM. Nevertheless, the

electrode of OAM/PEI (curve c) exhibited substantially much smaller semicircles, implying that the efficient interfacial electron transfer imparted by PEI could reduce the charge transport resistance due to the positively charged PEI with amino group could further support the transfer of negatively charged $[Fe(CN)_6]^{3-/4-}$. After Peptide@B-CQDs was immobilized on the electrode surface (curve d), the Ret increased owing to poor conductivity of B-CQDs and the insulating property of peptide produced hydrophobic films, blocking the electron transfer. After the electrode of OAM/PEI/Peptide@B-CQDs was incubated with the trypsin solution, the Ret value decreased due to trypsin specifically cleaved the site of the arginine that induced the partial peptide chains and B-CQDs were dropped off the electrode, reducing the electron-transfer resistance. This phenomenon revealed the practical feasibility of this PEC biosensor for trypsin detection.

The procedure of the proposed biosensor was then monitored via the stepwise transient photocurrent responses. As shown in Fig. 3B, the OAM modified electrode (curve b) exhibited an apparent photocurrent signal compared with the bare GCE (curve a), suggesting that OAM, as a newly typical photoactive species, possessed monstrous potential for PEC biosensing applications. With the PEI coated on (curve c), the OAM/PEI modified electrode submitted the maximal photoresponse, which demonstrated that PEI could trigger the rapid electrons transfer. Subsequently, the photocurrent intensity decreased dramatically after the Peptide@B-CQDs was anchored (curve d), which was ascribed to the immobilized bioconjugates suppressed the charge carriers transfer and the B-CQDs could competitively absorb light, leading to lower light absorption efficiency of OAM/PEI. When trypsin was subsequently incubated on the electrode, the photocurrent response was re-improving due to the short peptide sequence containing arginines could be hydrolyzed selectively by

trypsin and B-CQDs were fell off the electrode, and the impedance was released, enhancing the electrons transfer between the electrode and electrolyte. Thus, the photocurrent response of different modified electrodes confirmed the successful construction of the proposed biosensing strategy.

Fig. 3

3.4. The proposed PEC signal amplification strategy for the trypsin detection

Apart from the exploration of the basal photocurrent response, fabricating an efficient and amusive bioprobe was also crucial in hoisting the analytic performance and the sensitivity of PEC protein detection. In this "on-off-on" case, an attractive and promising probe, B-CQDs with good biocompatibility, was applied for labeling the peptide. To further certify the feasibility of this tag when applied in the trypsin monitoring, a comparison experiment was performed to elucidate the applicability of B-CQDs. As displayed in Fig. 4, both peptide (curve a) and Peptide@B-CQDs (curve a') anchored electrodes decreased the photocurrent response, however, the curve a' submitted a more apparent reduction, which indicated the B-CQDs with poor conductivity hindered the electrons transfer and simultaneously absorbed light illumination reducing the generation of the charge carriers. This outcome revealed that the B-CQDs were an efficient quencher to reduce the background signal and enhance the sensitivity further. When the trypsin was incubated on the electrodes, the photocurrent responses were coinstantaneously improved (curve b and b' in Fig. 4). Nevertheless, from the histogram inserted in Fig. 4, a remarkable contrast could be observed that the amplification deviation for Peptide@B-CQDs (pink) was larger than peptide (blue), confirming that B-CQDs was a viable option to assist the peptide for further signal depression in improving high sensitivity and wide linear range for this biosensor.

Fig. 4

3.5. Optimization of the PEC biosensing platform and experimental conditions

In order to acquire better analytical performance, the conditions of the biosensor fabrication including the amounts of OAM and PEI as well as the functionalization time between peptide (3.0 mg/mL) and B-CQDs (1.0 mg/mL) were measured. The optimal usage quantity was 1 mg/mL for OAM and 0.5 mg/mL for PEI (shown in Fig. S3A and S3B). It could be explained that more electrons could be excited with the OAM concentration increasing, causing the enhancement of photocurrent density. However, the thicker OAM film would gather together, which impeded the transfer of the electrons and the effective light harvest, leading to the photocurrent decreased. Thus, the optimum conditions of OAM were determined to be 1.0 mg/mL. Additionally, as exhibited in Fig. S3B, the photocurrent density gradually increased with the increasing amount of PEI from 0.3 to 0.5 mg/mL, ascribing to particular features of PEI that accelerated the electrons transfer. Subsequently, the photocurrent descend because the excessive PEI resulted in thicker film, causing the internal resistance and photocurrent descended. Therefore, 0.5 mg/mL was selected for the subsequent measurements. The functionalization time between peptide and B-CQDs incubation time of was 10 h. As illustrated in Fig. S3C, with the absorption time increasing, the photocurrent density decreased due to the more visible light was absorbed by B-CQDs as well as the steric hindrance effect of peptide chains. For the sake of a significant photocurrent signal and higher sensitivity, 10 h was chosen as the optimized time for the signal recording in the following experiments. Additionally, several experimental parameters such as trypsin incubation time, absorption time of Peptide@B-CQDs, pH value and the applied potential were also investigated (Fig. S4). The incubation time for trypsin and peptide@B-CQDs were 60 min and 50 min,

respectively. Finally, the measurements were performed in PBS pH 7.4 and applied potential of 0 V. The detailed explication was displayed in the supporting information.

3.6. Analytical performance of the "on-off-on" biosensor

Under the optimal conditions, the proposed PEC bioassay was utilized to detect the trypsin standards with different concentrations. As presented in Fig. 5A, the degree of signal increment was directly related to the increasing trypsin amount. A linear relationship between the photocurrent density and the logarithmic values of trypsin concentration was obtained, which was shown in Fig. 5B. The linear regression equation of the calibration curve was j ($\mu A\ cm^{-2}$) = 0.07326 log C (mg/mL)+0.92228 with R^2=0.9943 in the dynamic range of 10^{-7}-1.0 mg/mL, and the limit of detection (LOD) was 0.32×10^{-7} mg/mL, which was sufficiently low for pathological conditions monitoring. Appreciatively, the detection range and the LOD compared with other previous reports were presented in Table S1 (Supporting information). Additionally, the practicability of this strategy was investigated on real sample of human serum with recovery rate of 97.3-100.8 % (Table S2).

Fig. 5

3.7. Specificity, reproducibility, and stability of the PEC biosensor

To investigate the selectivity of the "on-off-on" PEC bioassay, the photocurrent response was evaluated against other common enzymes such as lysozyme (Lys), horseradish peroxidase (HRP), glucose oxidase (GOx) and the corresponding mixture with trypsin (Try). As indicated in Fig. 5C, only the presence of target trypsin caused a stronger photocurrent in comparison with the blank signal, regardless of mixture with trypsin or alone. Such a high specificity could be attributed to the specific cleavage site of arginine in the substrate peptide chains.

Both intra-assay and inter-assay precision of the PEC biosensor were assessed.

The relative standard deviations (RSD) of intra-assay were 2.62% and 1.98% at 0.1 and 10^{-3} mg/mL, respectively. The inter-assay RSD of 3.24% and 2.96% were obtained by measuring the same trypsin samples of ten electrodes prepared separately at identical experimental conditions. These outcomes indicated the fine reproducibility of this PEC biosensor.

The stability of the biosensor was examined (Fig. 5D) and no obvious change of photocurrent density was observed within 200 s under interrupted light excitation, suggesting a good stability of this PEC bioassay. In addition, the biosensing electrode of OAM/PEI/Peptide@B-CQDs was stored in a humid and dark environment at 4 °C before further measurement. After twelve days, the photocurrent response still remained 94.8% of its initial value, demonstrating the excellent long-term storage stability and long-standing lifetime. As a proof of principle, these preliminary results revealed the feasibility of this protocol for the sensitive trypsin assay.

3.8. The inhibition effect of trypsin inhibitor

It is well known that the trypsin inhibitors could restrain the cleavage of arginine sites by inactivating trypsin. Correspondingly, the photocurrent density would decline while the inhibitors were present in the trypsin solution. A Bowman-Birk inhibitor (BBI) extracted from the soybeans was chosen to validate the practicability of this PEC biosensor. The IC_{50} value (the concentration of the inhibitor that caused 50% inhibition of the trypsin activity) of BBI toward trypsin was assessed to be 0.3 μg/mL (Fig. 6), which was lower than the previous report (Xue et al. 2011). After the experimental verification, these results obviously manifested that this PEC protease bioassay was facilely accessible and could be applied for proteases activity detection and the inhibitor-screening.

Fig. 6

4. Conclusion

In summary, an ultrasensitive and simple PEC strategy for protein trypsin detection was established based on the PEI sensitized multifunctional OAM as the biosensor matrix coupled with B-CQDs labeled peptides as signal quenchers. Herein, on account of the strong absorption capacity of OAM, PEI was absorbed onto the OAM modified electrode surface to expedite the electrons transfer, which noticeably improved the photocurrent response. As the bioprobes, Peptide@B-CQDs conjugates could dramatically weaken the photoresponse owing to the competitive harvest of exciting light and the obvious steric hindrance of this bioconjugates. Moreover, the recognition-induced structure change of peptide by trypsin re-promoted the photoelectric signal due to the arginine-containing site on peptide was cleaved by trypsin, resulting in partial peptide chains and B-CQDs deviated from the electrode. With these motivations, a useful "on-off-on" PEC scheme for practical application in quantitative trypsin activity assay was fabricated, which could be a versatile protocol for proteases monitoring in life science and biological research.

Acknowledgements

This project was financially supported by the NSFC (21205016, 21575024), National Science Foundation of Fujian Province (2016J06003, 2016J05026), Education Department of Fujian Province (JA14071, JB14036, JA13068) and Foundation of Fuzhou Science and Technology Bureau (2015-S-160, 2015-G-72) and New Century Talent Project of Fujian Province.

References

Bisquert, J., Zaban, A., Greenshtein, M., Mora-Seró, I., 2004. J. Am. Chem. Soc. 126 (41), 13550-13559.

Chen, Q., Liu, H., Xin, Y., Cheng, X., Li, J., 2013. Appl. Surf. Sci. 264, 476-484.

Chen, Y., Ding, J., Qin, W., 2012. Bioelectrochemistry 88, 144-147.

Chen, Y., Huang, W., He, D., Situ, Y., Huang, H., 2014. ACS Appl. Mater. Interfaces 6 (16), 14405-14414.

Choi, H., Park, J. S., Jeong, E., Kim, G. H., Lee, B. R., Kim, S.O., Song, M. H., Woo, H.Y., Kim, J.Y., 2011. Adv. Mater. 23 (24), 2759-2763.

Dai, H., Zhang, S., Gong, L., Li, Y., Xu, G., Lin, Y., Hong, Z., 2015. Biosens. Bioelectron. 72, 18-24.

Ge, L., Wang, P. P., Ge, S., Li, N. Q., Yu, J. H., Yan, M., Huang, J. D., 2013. Anal. Chem. 85 (8), 3961-3970.

Hong, M. L., Li, L. J., Han, H. X., Chu, X., 2014. Anal. Sci. 30 (8), 811-815.

Kang, H., Hong, S., Lee, J., Lee, K., 2012. Adv. Mater. 24 (22), 3005-3009.

Kongkanand, A., Tvrdy, K., Takechi, K., Kuno, M., Kamat, P. V., 2008. J. Am. Chem. Soc. 130 (12), 4007-4015.

Li, Y. J., Ma, M. J., Zhu, J. J., 2013. Anal. Chem. 84 (23), 10492-10499.

Liu, Y. F., Chen, J. X., Xu, M. Q., Zhao, G. C., 2014. Int. J. Electrochem. Sci. 9 (7), 4014-4023.

Liu, Z., Li, Y., Zhao, Z., Cui, Y., Hara, K., Miyauchi, M., 2010. J. Mater. Chem. 20 (3), 492-497.

Pan, J. H., Lee, W. I., 2006. Chem. Mater. 18 (3), 847-853.

Rhodes, M. B., Hill, R.M., Feeney, R. E., 1957. Anal. Chem. 29 (3), 376-378.

Shan, X., Chai, L., Ma, J., Qian, Z., Chen, J., Feng, H., 2014. Analyst 139 (10), 2322-2325.

Song, X. M., Wu, J. M., Tang, M. Z., Qi, B., Yan, M., 2008. J. Phys. Chem. C 112 (49), 19484-19492.

Wang, X., Li, S., Zhang, P., Lv, F., Liu, L., Li, L., Wang, S., 2015. Adv. Mater. 27, 6040-6045.

Xue, W., Zhang, G., Zhang, D., 2011. Analyst 136 (15), 3136-3141.

Yan, K., Liu, Y., Yang, Y., Zhang, J., 2015. Anal. Chem. 87 (24), 12215-12220.

Yang, D., Fu, P., Zhang, F., Wang, N., Zhang, J., Li, C., 2014. J. Mater. Chem. A 2 (41), 17281-17285.

Zhang, W., Zhang, P., Zhang, S., Zhu, C., 2014. Anal. Methods 6 (8), 2499-2505.

Zhao, W. W., Xu, J. J., Chen, H. Y., 2014. Chem. Rev. 114 (15), 7421-7441.

Zheng, F. F., Wu, J. F., Zhao, G. C., 2012. Anal. Methods 4 (12), 3932-3936.

Zhou, L., Smyth Boyle, D., O'Brien, P., 2007. Chem. Commun. (2), 144-146.

Figure captions

Scheme 1 (A) Fabrication procedure and (B) the mechanism of this PEC biosensor.

Fig. 1 (A) SEM and (B) HRTEM images of OAM nanoparticles. The insets in A and B were the N_2 adsorption-desorption isotherms and XRD patterns of OAM. (C) HRTEM image and (D) UV-vis and fluorescence spectra of B-CQDs.

Fig. 2 (A) Applied potential bias-dependent photocurrent densities under light on/off illumination, (B) IPCE spectra at applied potential of 0 V, (C) Voc time profile and (D) electron lifetimes measurements (determined from the Voc decay in dark) of (a) OAM and (b) OAM/PEI in 0.1M PBS (pH 7.0).

Fig. 3 (A) EIS spectra and PEC response of different modified electrodes. (a) GCE, (b) GCE/OAM, (c) GCE/OAM/PEI, (d) GCE/OAM/PEI/Peptide@B-CQDs, (e) the electrode of (d) incubated with trypsin (0.1 mg/mL). The concentration of peptide was 3mg/mL.

Fig. 4 (A) Photocurrent densities of different electrodes: (a) OAM/PEI/Peptide, (b) the electrode of (a) incubated with trypsin, (a') OAM/PEI/Peptide@B-CQDs, (b') the electrode of (a') incubated with trypsin. The concentrations of peptide and trypsin were 3mg/mL and 0.1 mg/mL, respectively.

Fig. 5 (A) Photocurrent responses of trypsin standards with different concentrations (a-h) 10^{-7}-1.0 mg/mL. (B) The corresponding calibration curve. (C) Selectivity of the proposed assay of trypsin (10^{-4} mg/mL) determined by comparing with interfering agents, including 10^{-2} mg/mL HRP, GOx, Lys and the corresponding mixed solutions. (D) Time-based photocurrent density of GCE/OAM/PEI/Peptide@B-CQDs/trypsin measured with light switched on and off.

Fig. 6 Plot of the inhibition efficiency of trypsin inhibitor versus the concentration of inhibitor.

Scheme 1

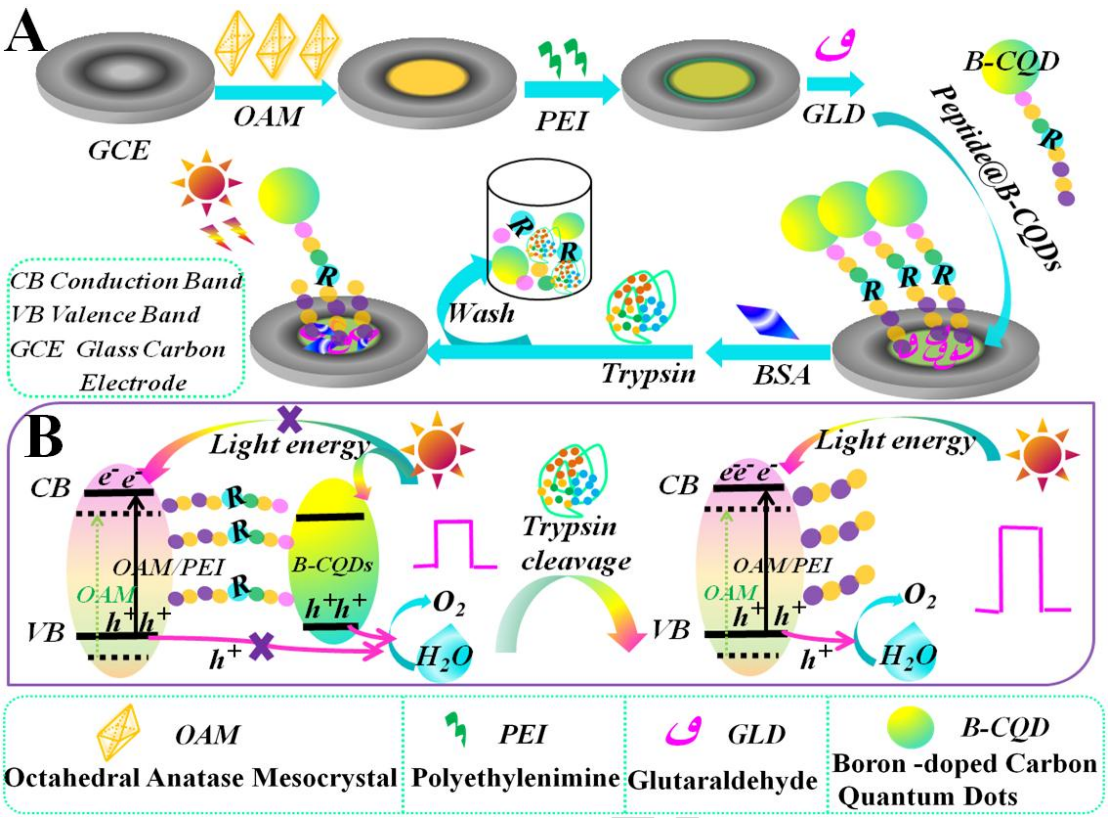

Figure 1

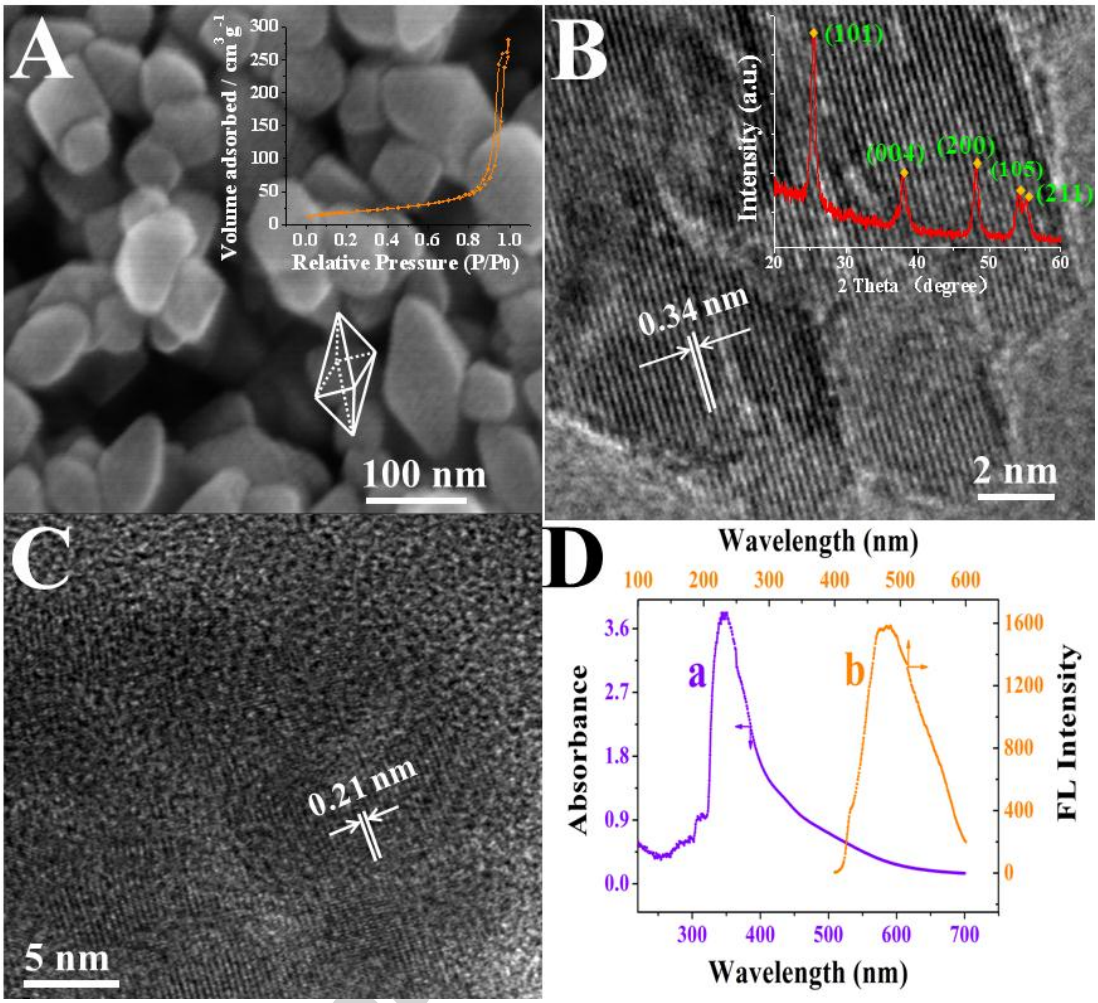

Figure 2

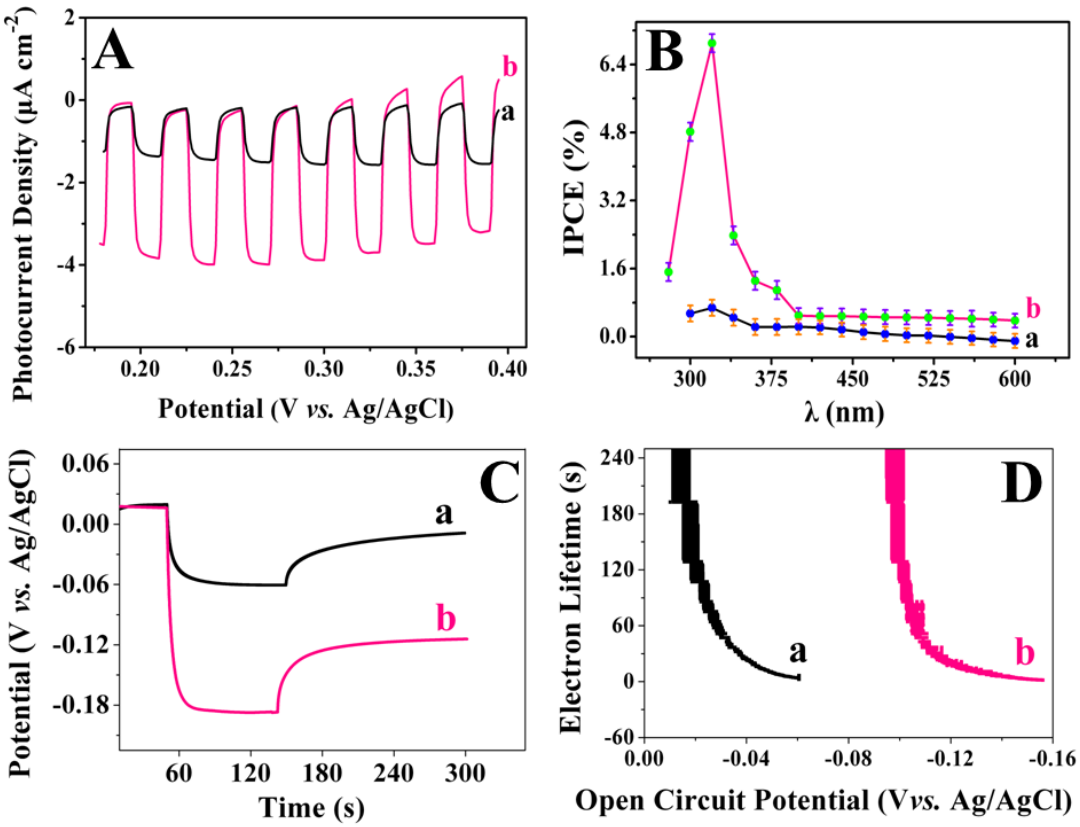

Figure 3

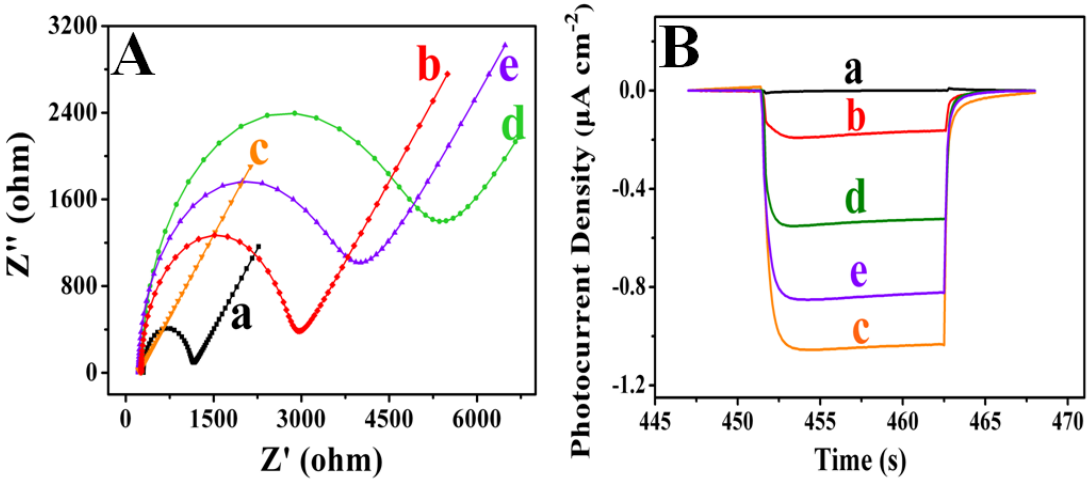

Figure 4

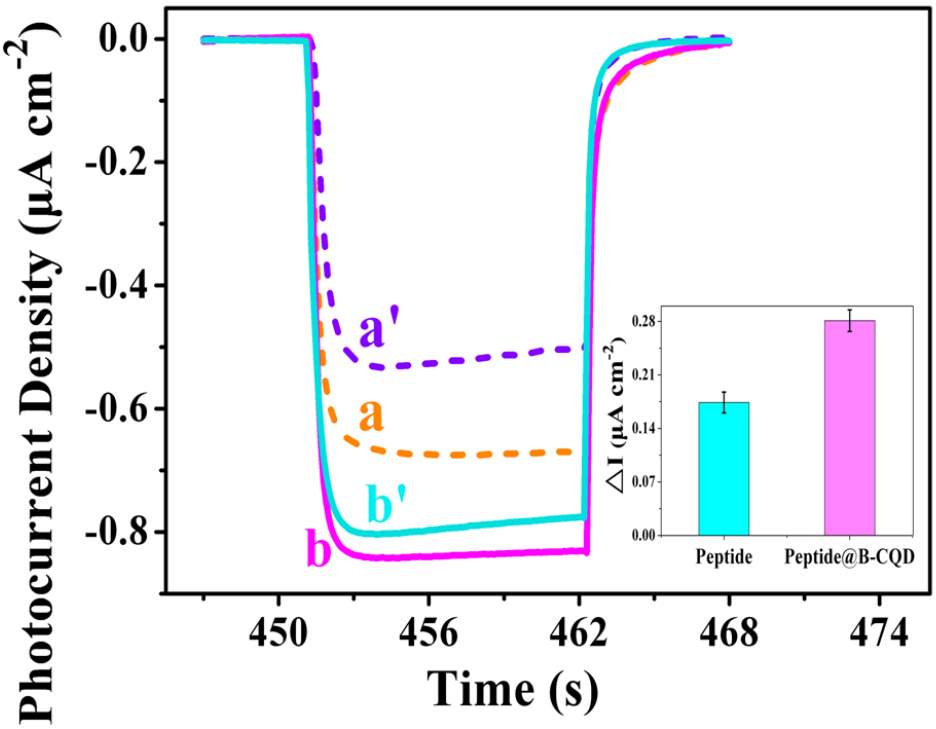

Figure 5

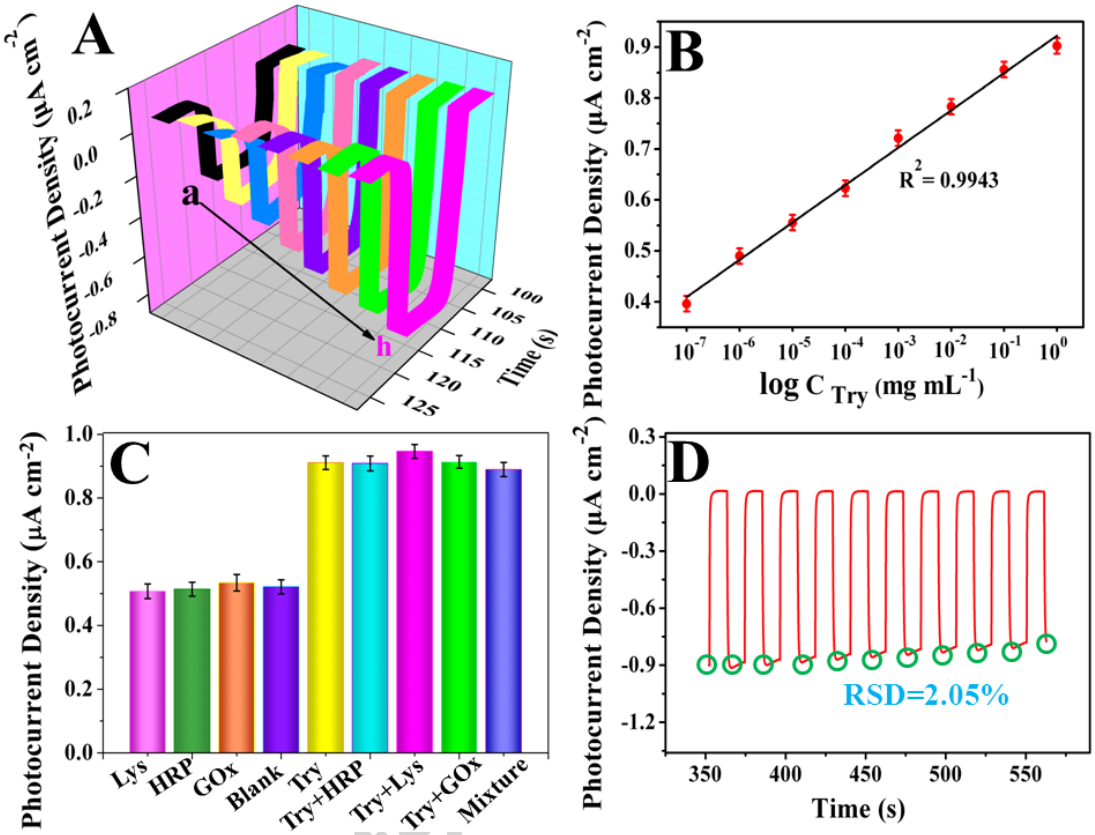

Figure 6

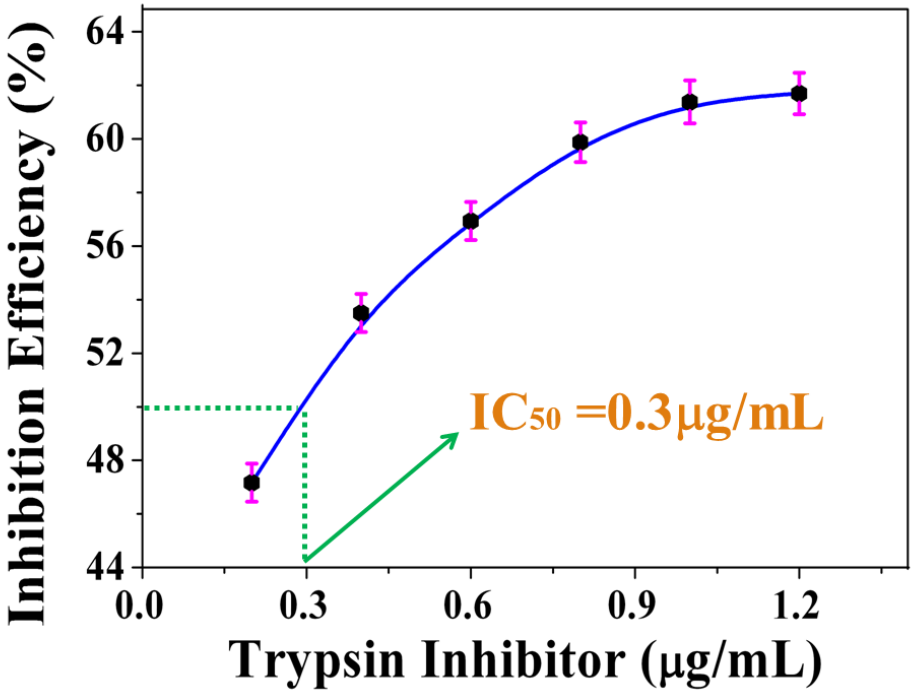

Highlights

- An efficient photoelectrochemical strategy was designed for trypsin detection.
- Polyethylenimine decorated TiO_2 mesocrystal were used as photoactive matrix.
- Boron-doped carbon dots further elevated sensitivity by labeling on the peptide.